Chapter 2

Experimental Methods:

Material Synthesis, Analysis with Device Fabrication, and Performance Evaluation

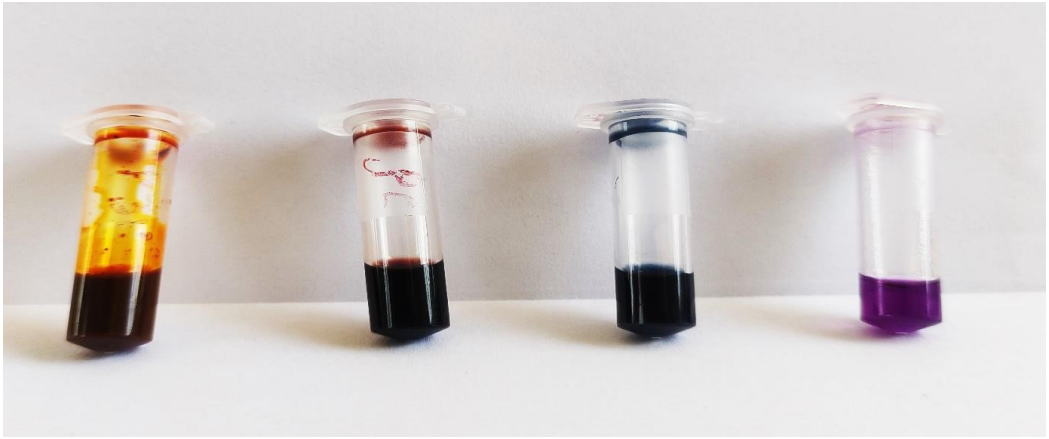

Chapter 2

In this chapter, I explore a variety of experimental methodologies integral to this thesis, including materials synthesis, characterization techniques, device fabrication processes, and device performance assessments. The materials synthesis section highlights three distinct approaches for producing ion-conducting oxide dielectrics, metal oxide semiconductors, and organic polymeric materials. The characterization of these materials, primarily in thin-film form, encompasses a comprehensive suite of analytical techniques. The device fabrication section covers the development of thin film heterostructure photodetectors, transparent conductors, transparent heat reflectors, SERS substrate, and organic photovoltaics. Finally, the electrical characterization focuses on critical analyses, including current-voltage (I-V), current-time (I-t), EQE, and SERS measurement, offering key insights into device behavior and performance.

2.1 Materials Synthesis

In this thesis work, mainly three different types of materials have been synthesized via low-cost solution process method. These materials have included i) ion-conducting dielectric, ii) metal-oxide semiconductor, and iii) organic polymeric materials. The ion-conducting dielectric material is used as an initial material to synthesize plasmonic Ag-TiO_2 thin films. Various kinds of metal oxide semiconductors like SnO_2, SnO_2 NPs, ZnO, ZnO NPs, TiO_2 and TiO_2 NPs have been synthesized for different device applications. A non-conducting polymer, polymethyl methacrylate (PMMA), has been used as a protective layer for some particular devices. Organic dye rhodamine 6G (R6G) and vitamin B_{12} have been used as analytic molecules for SERS experiments. Organic polymer poly(3-hexylthiophene) (P3HT) and [6,6]-phenyl-C_{71}-butyric acid methyl ester ($PC_{71}BM$) are used as an active material. Conducting polymer poly(3,4-ethylenedioxythiophene) polystyrene sulfonate (PEDOT: PSS) is used as a HTL for the fabrication of photovoltaic devices. The solution process

method allows uniform molecular-level reactions, which allow single-compound thin film formation. The detailed synthesis process is outlined below.

2.1.1 Synthesis of Ion-Conducting Dielectric $Li_4Ti_5O_{12}$ Precursor Solution

An ion-conducting dielectric ($Li_4Ti_5O_{12}$) thin film has been deposited on a plastic substrate by a solution-processed technique. A two-step process has been adapted to produce a thin layer of $Li_4Ti_5O_{12}$. Initially, we take lithium acetate dihydrate [$LiOOCCH_3.2H_2O$] (acquired from Alfa-Aesar, 99% extra pure] and titanium (IV) butoxide [$Ti(OC_4H_9)_4$] (acquired from Sigma-Aldrich, >97% pure) as precursor chemicals. Different molarity solutions of both are prepared in 2-methoxy ethanol (2-MEA) solvent and stirred each for 1 h at 700 r.p.m, and then both solutions are added in a 4:5 volume ratio to prepare a precursor solution of $Li_4Ti_5O_{12}$ ceramic product. The mixture is then vigorously stirred for the next 1 h at 700-800 r.p.m under ambient atmospheric conditions to yield a clear, transparent, and homogeneous solution. The synthesis step is schematically present in **Figure 2.1**.

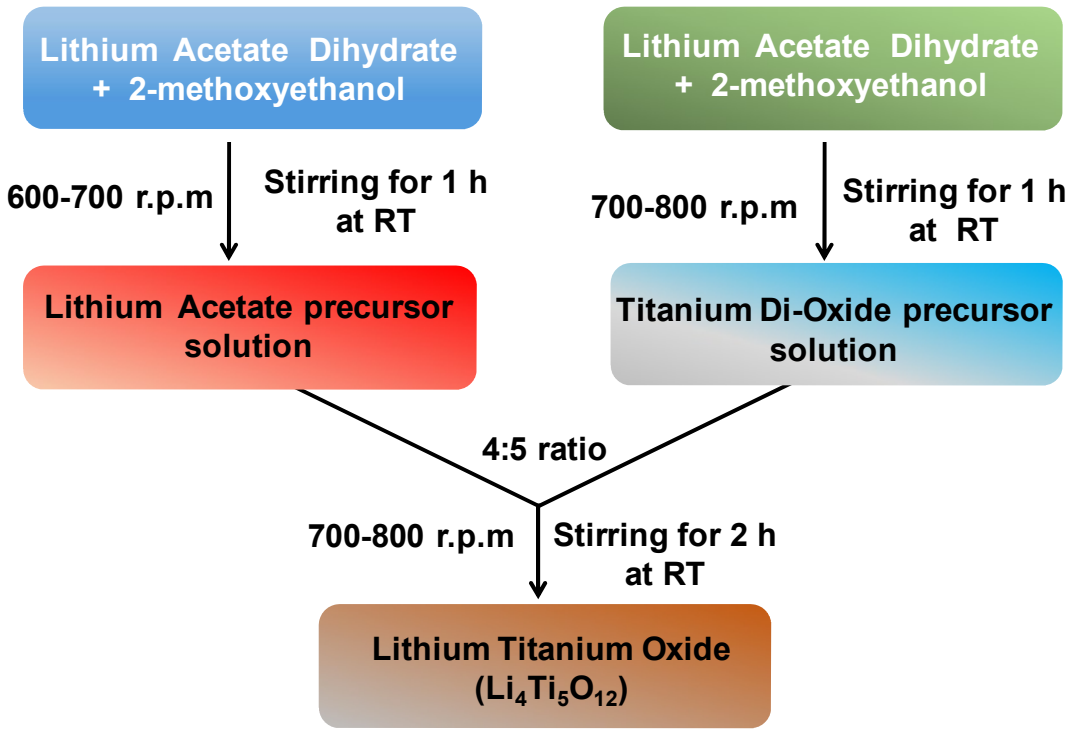

Figure 2.1 Synthesis of ion-conducting dielectric $Li_4Ti_5O_{12}$ by solution process route.

2.1.2 Synthesis of SnO_2 Precursor Solution

The Solution process SnO_2 has been employed as a metal-oxide semiconductor channel layer for photodetector fabrication. Different concentration precursor solution has been prepared by dissolving tin chloride [$SnCl_2$] (99.99%, obtained from Sigma Aldrich) in 2-MEA solvent, and the solutions are stirred for 30 minutes at 700-800 r.p.m before spin coating.

2.1.3 Synthesis of Precursor Solution of SnO_2 NPs

For the synthesis of SnO_2 NPs, at first, a required amount of tin chloride is mixed in distilled water to make 300 mM concentration precursor solution. During this solution preparation, cetrimide (Cetyl Trimethyl Ammonium Bromide) (CTAB) (purchased from Aseschem) is added that works as a reacting agent. This mixture was then stirred for 2 h to obtain a clear solution. To grow SnO_2 NPs, sodium borohydrate (NaBH4, 98% extra pure crystals, purchased from SRL) are added in this solution dropwise that forms a white precipitation of SnO_2 NPs. White part of this mixture is then cleaned by a centrifuge at 10000 r.p.m for 5 minutes and dried in a preheated hot plate at 60˚C for overnight. Then SnO_2 NPs are dispersed it in methanol to make the final SnO_2 NPs solution. Detailed synthesis process is schematically present in **Figure 2.2**.

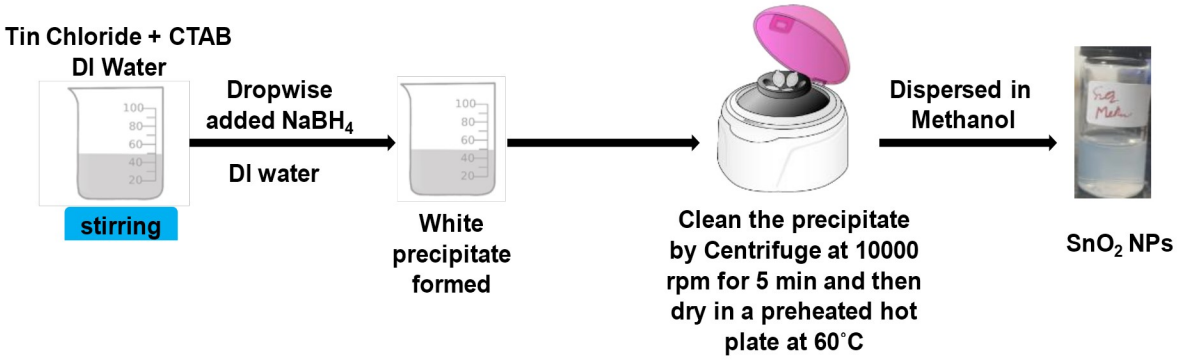

Figure 2.2 Schematic representation for the synthesis of SnO_2 NPs by solution process method.

2.1.4 Synthesis of Precursor Solution of ZnO NPs

For the preparation of colloidal ZnO NPs with a concentration of 20 mg/ml, zinc acetate dihydrate (purchased from Sigma-Aldrich, 99% pure) and potassium hydroxide (KOH) have been selected as the precursor salts. Each salt is individually dissolved in methanol and heated at 60°C for 10 min. The KOH solution is then injected into the Zinc acetate solution, resulting in the rapid clouding of the mixture. After 30 minutes, it clarified and stirred for 3 h at the same temperature. The solution is left undisturbed for 4 h to allow particle precipitation under normal atmospheric conditions. The clear top solution is carefully decanted, redissolved in methanol, and set aside for 16 h. The subsequent steps involve centrifuging the solution with the addition of acetone and rinsing with methanol, repeated three times. Finally, methanol is added to the remaining NPs in the centrifuge tube, followed by sonication. After allowing for any precipitation, the top solution constitutes the synthesized colloidal ZnO NPs. Detailed synthesis process is schematically present in **Figure 2.3**.

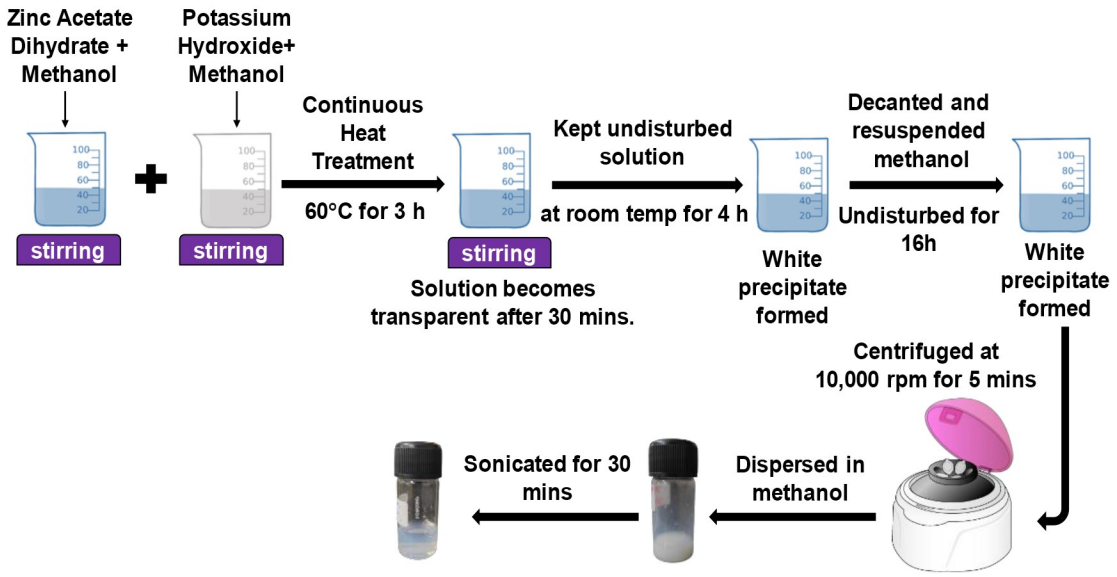

Figure 2.3 Schematic representation for the synthesis of ZnO NPs by solution process method.

2.1.5 Synthesis of Precursor Solution of TiO_2

To prepare the TiO_2 thin film via sol-gel method, 100 mM concentration of titanium (IV) butoxide [$Ti(OC_4H_9)_4$] (acquired from Sigma-Aldrich, >97% pure) solution is prepared by dissolving it in 2-MEA solvent and stirred at room temperature around 30 min at 600 r.p.m to prepare a transparent precursor solution.

2.1.6 Preparation of Precursor Solution of TiO_2 NPs

For the preparation of TiO_2 NPs, 18NR-T transparent titanium paste has been used as a source material which is dispersed in ethanol to prepare a colloidal solution of concentration 100 mg/ml. A stable colloidal solution is obtained after mixing it through an ultra-sonication process for 30 minutes. Then the solution is left for 10 minutes at room temperature before spin coating.

2.1.7 Preparation of PMMA Solution

A PMMA precursor solution is prepared by dissolving powder of PMMA (Sigma-Aldrich, molecular weight ~350,000), in chloroform solvent (SRL, extrapure AR). The dissolved process involved vigorous magnetic stirring at 1200 r.p.m for 4-5 h at room temperature. Subsequently, the prepared solution has been left undisturbed for 30 minutes to stabilize the solution before spin coating.

2.1.8 Preparation of PEDOT: PSS Solution

1.2 WT% of PEDOT; PSS solution is prepared by adding 80 ml DI water with pure solution and then sonicate it for 1 hr. using ultra-sonicator for 30 min. The solution is then stored in a cool & dark place before spin coating.

2.1.9 Preparation of P3HT Solution

Solution of P3HT polymer is prepared by dissolving the required amount of P3HT powder (Sigma-Aldrich) in chlorobenzene (Sigma-Aldrich). Prepared solution is stirred at 600-700 r.p.m at 60˚C for 1 h and then probe sonicate for 5 min to ensure proper mixing before spin coating the solution.

2.1.10 Preparation of $PC_{71}BM$ Solution

Solution of $PC_{71}BM$ organic polymer is prepared by dissolving the required amount of $PC_{71}BM$ powder (Sigma-Aldrich) in chlorobenzene solution. Prepared solution is probe sonicate for 30 min to ensure proper mixing.

2.1.11 Preparation of blended P3HT: $PC_{71}BM$ Solution

Solution of P3HT and P3HT: $PC_{71}BM$ are blended (1:1 ratio) in the same wt % and then probe sonicate it for 1 hr. at room temperature for proper mixing. After that, the mixture is stored at a cool and dark place for 20 min before use.

2.1.12 Solution Preparation of R6G Dye & Vitamin B_{12} Biomolecules

A parent solution with concentrations of 10^{-3} M for R6G and vitamin B_{12} is prepared using Milli-Q water. This solution is prepared through ultrasonic processing for a duration of 4-5 hours at ambient temperature. Subsequently, through the method of serial dilution, the concentrations of R6G and vitamin B_{12} are varied in the range from 10^{-6} M to 10^{-12} M which are derived from their respective initial concentration.

2.2 Substrate Cleaning Process

In device fabrication, the substrate cleaning process is a critical initial step to ensure the removal of contaminants from the surface of materials like silicon wafers, glass or plastic substrates. Effective cleaning is vital for the success of subsequent fabrication stages. The subsequent sections provide an explanation of the cleaning process for all the devices used in this thesis.

2.2.1 Glass Substrate Cleaning

For the device fabrication, borosilicate glass has been utilized as substrate. A widely adopted glass cleaning process is illustrated in the flow chart presented in **Figure 2.4**. At the beginning glass substrates of size 15 mm ×15 mm are kept inside piranha solution (concentrated H_2SO_4 and H_2O_2 in a 3:1 ratio) for 15 min to eliminate organic residues from the substrate's surface.[138] The substrates are then washed by using DI water for 10 minutes

with the help of an ultrasonic bath. Subsequently, substrates are transferred to a 2-propanol solution and kept inside an ultrasonic bath for 10 minutes, followed by a drying process with an air-blower.

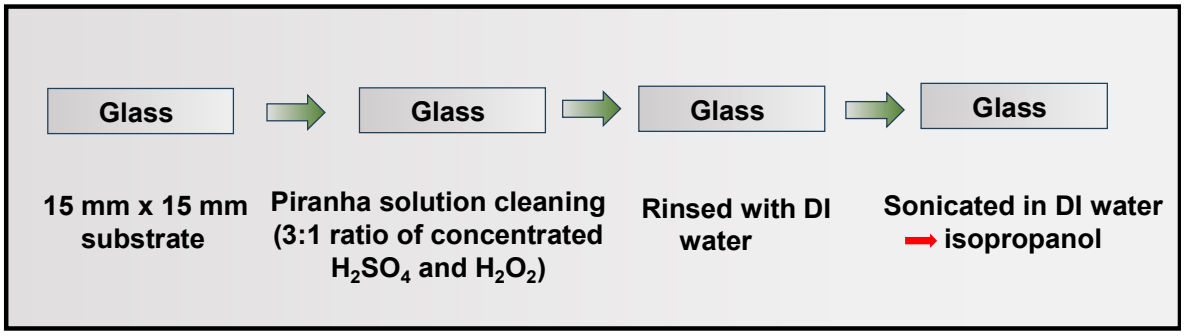

Figure 2.4 Schematic presentation of three-step solution cleaning of glass substrates.

2.2.2 Silicon Substrate cleaning

For the fabrication of thin-film devices, highly n-doped Si (n^+-Si) is also used as both substrates and bottom electrodes. For cleaning, a widely used three- step solution cleaning process is adopted, illustrated in **Figure 2.5**. Initially, the surfaces are cleaned with a soap solution (Extran) and subsequently rinsed with DI water. Following this, the substrates undergo a series of steps involving immersion in different media (such as DI water, acetone, and isopropanol) and ultra-sonication for 10 minutes in each step. The substrates are then dried by passing air and placed in a plasma cleaning chamber at 20 W for 10 minutes.[139] Plasma treatment enhances the hydrophilic nature of the surface and also removes residual organic materials, ensuring the fabrication of pinhole-free films.

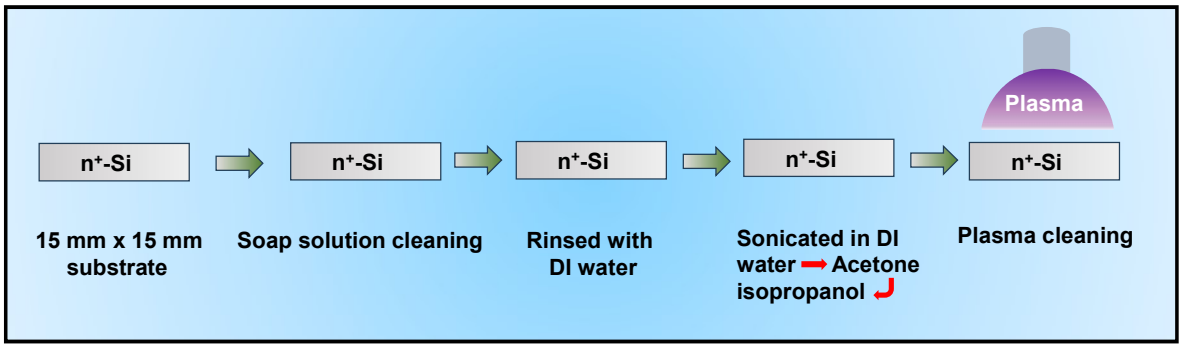

Figure 2.5 Schematic presentation of four-step solution cleaning step of traditional silicon cleaning followed by plasma treatment.

2.2.3 PET Substrate Cleaning

For flexible device fabrication, plastic PET substrates are used, and its step-by-step cleaning process is identical like silicon substrate cleaning process. At first, plastic substrate is cleaned with soap solution and then ultra-sonicate those substrates by DI water, acetone and isopropanol respectively each for 15-20 minutes. After that, the substrates are dried properly with an air-blower. Then those dried substrates are placed in an oxygen plasma cleaner at 20 W power for 10 minutes. This process is highly effective in removing organic and inorganic residues from the substrate's surface.

2.3 Device Fabrication

The subsequent sections provide a brief outline of all different device fabrication process used in this thesis.

2.3.1 Ag-TiO_2 Based Heterostructure Photoconductor

This photodetector has been fabricated on a glass substrate in a photoconductor geometry and the fabrication steps of this device has been shown schematically in **Figure 2.6**. At first, glass substrates are cleaned, and the cleaning process is described in **Section 2.2.1**. These clean glass substrates are spin-coated with a 300 mM SnO_2 precursor solution for 40 s at 4000 rpm and transferred on a preheated hot plate at 100°C. The substrates are then annealed for half an hour at 500°C to form the crystalline SnO_2 thin film. To get the desired thickness of SnO_2 layer, this process is repeated 3 times. A TiO_2 layer is then deposited on top of the SnO_2 film in a similar process. Therefore, the precursor solution of TiO_2 is spin-coated for 50 s at 5000 rpm and annealed at 500°C for 30 min to grow a highly crystalline layer. The photoactive Ag-TiO_2 nano-Schottky junction thin film has been grown on top of this glass/SnO_2/TiO_2 substrate. For this Ag-TiO_2 thin film deposition, antecedent solution of LTO is spin-coated over these substrates for 30 s at 3000 rpm and then annealed at 550°C for 1 hr. to form a crystalline surface. Those crystallization films are submerged in a 100 mM $AgNO_3$ solution for 1 hr. to exchange Li^+ of LTO film with Ag^+ of the solution that forms $Ag_4Ti_5O_{12}$. Following this ion-exchange procedure, the samples are rinsed with DI water to eliminate any remaining $AgNO_3$ from the surface of the film. After washing, the substrates are immersed in a 300 mM $NaBH_4$ solution at ambient temperature for 1 hr. which changes

the color of the substrate from transparent to yellowish. Throughout this process, Ag^{+} has been transformed to metallic silver (Ag^{0}) to make Ag-NPs, and the initial $Ag_4Ti_5O_{12}$ crystal is transformed to TiO_2 to form the final Ag-TiO_2 nano-Schottky junction thin film. **Equations** (**2.1** & **2.2**) show the chemical processes of this ion exchange and reduction procedure, respectively. After reduction, the films are cleaned by dipping inside DI water to eliminate any remaining $NaBH_4$ solution from the surface of the film.[140] Finally, silver electrodes (electrode area ~ 0.84×0.84 mm^2) are deposited by thermal evaporation on top of this glass/SnO_2/TiO_2/Ag-TiO_2 film through a shadow mask process.

Ion-exchange and reduction reaction:

$$Li_4Ti_5O_{12} + 4\,AgNO_3 \xrightarrow{Li^{+} \longrightarrow Ag^{+}} Ag_4Ti_5O_{12} + 4\,LiNO_3 \qquad \text{-------} \quad (2.1)$$

$$Ag_4Ti_5O_{12} + NaBH_4 \xrightarrow{Ag^{+} \longrightarrow Ag^{0}} 4Ag\text{-}5TiO_2 + NaBO_2 + 2H_2 \qquad \text{------} \quad (2.2)$$

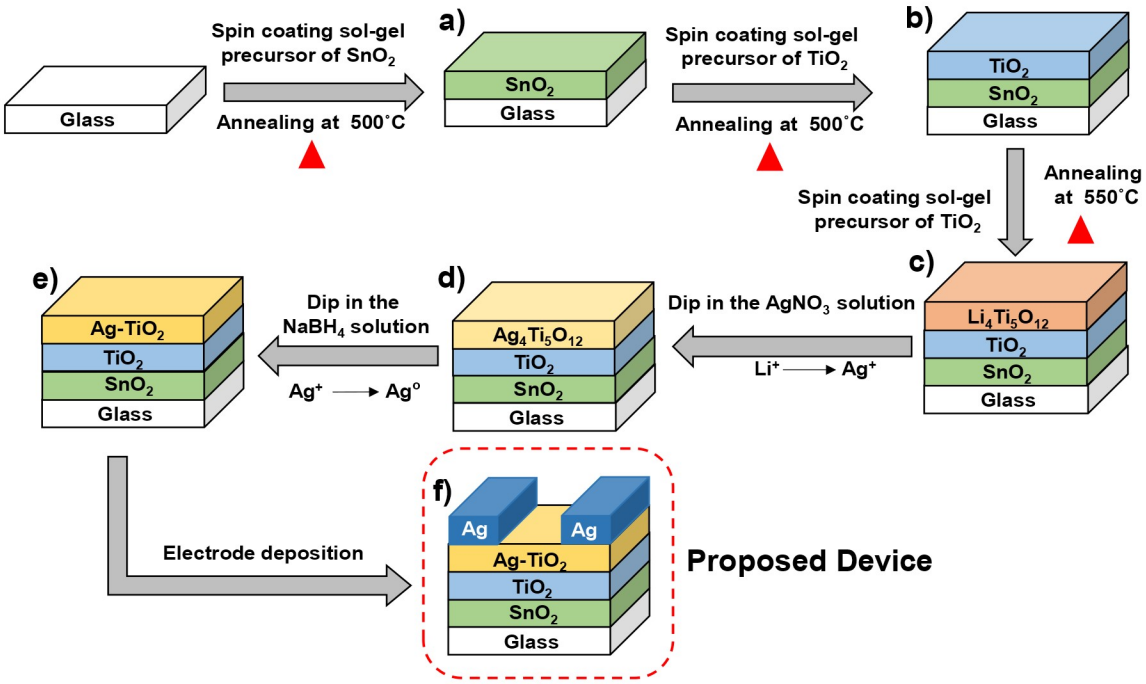

Figure 2.6 Depicts the six-step growth process of an in situ grown Ag-TiO_2 thin film-based photodetector : **a)** SnO_2 thin layer on glass substrate via spin coating of a sol-gel precursor followed by annealing **b)** spin coating of TiO_2 thin film precursor followed by annealing at 500°C **c)** spin coating of LTO precursor and 1 hr. annealing at 550 °C to achieve polycrystalline LTO thin film **d)** Li^{+} ions are exchanged with Ag^{+} ions in an ion-exchange

process to form $Ag_4Ti_5O_{12}$ **e)** reduction process which reduces Ag^+ ions into Ag^0 to form Ag-TiO_2 thin film containing Ag NPs inside the TiO_2 matrix **f)** finally Ag electrode is deposited on top for electrical contact.

2.3.2 Ag/Ag-TiO_2 based Transparent Conductor (TC) & Transparent Heat Reflector (THR) Film

The TC & THR thin film has been fabricated on a plastic PET substrate which is schematically presented in **Figure 2.7**. In this fabrication process, at the beginning, plastic substrates (20×20 mm^2) are cleaned, and cleaning process is mentioned in **Section 2.2.3**. Then the precursor solution of LTO is spin-coated over the clean substrates for 30 s at 3000 rpm and immediately kept on a hot plate at 100°C. Subsequently, UV light of intensity ~ 9 W/m^2 is illuminated from that top side of the hotplate and keep it for 1 hr. This combined heating and UV illumination enable us to deposit crystalline LTO thin film at 100°C. However, without using UV light, it is required 550°C annealing to achieve this crystalline phase of LTO where we can't use common plastic PET as a substrate. These crystalline LTO films are then immersed in a 100 mM $AgNO_3$ solution for 1 hr. where Ag^+ of the solution are exchanged with Li^+ of the film that convert LTO thin film to $Ag_4Ti_5O_{12}$ thin film which subsequently convert to Ag-TiO_2 film due to the formation of Ag cluster inside oxide film. The reduction of Ag^+ to Ag^0 occurs due to the unstable nature of $Ag_4Ti_5O_{12}$. Moreover, the residual part of the oxide film also converted to TiO_2, resulting an Ag-TiO_2 thin film. These individual Ag NPs and TiO_2 phases have been identified through XRD study which is discussed later. Following the ion-exchange process, the samples are rinsed with DI water to wash any excess $AgNO_3$ from the film's surface. The chemical reaction of this process is illustrated in **Equation 2.3**. After that, 10 nm Ag thin film is deposited on the top of the Ag-TiO_2 thin film using a thermal evaporator to get a TC or THR film. Finally, a very thin layer of PMMA polymer is deposited over the 10 nm Ag/Ag-TiO_2 film by the spin-coating method (75 mg/mL,1000 rpm for 30 s) to provide better chemical and air stability of the prepared film.

Ion-exchange reaction:

$$Li_4Ti_5O_{12} + 4AgNO_3 \xrightarrow{Li^+ \longrightarrow Ag^+} Ag_4Ti_5O_{12}\ (\text{unstable}) + 4LiNO_3 \quad \text{-------} \quad (2.3)$$

$$Ag_4Ti_5O_{12}\ (\text{unstable}) \longrightarrow Ag\text{-}TiO_2\ (\text{stable})$$

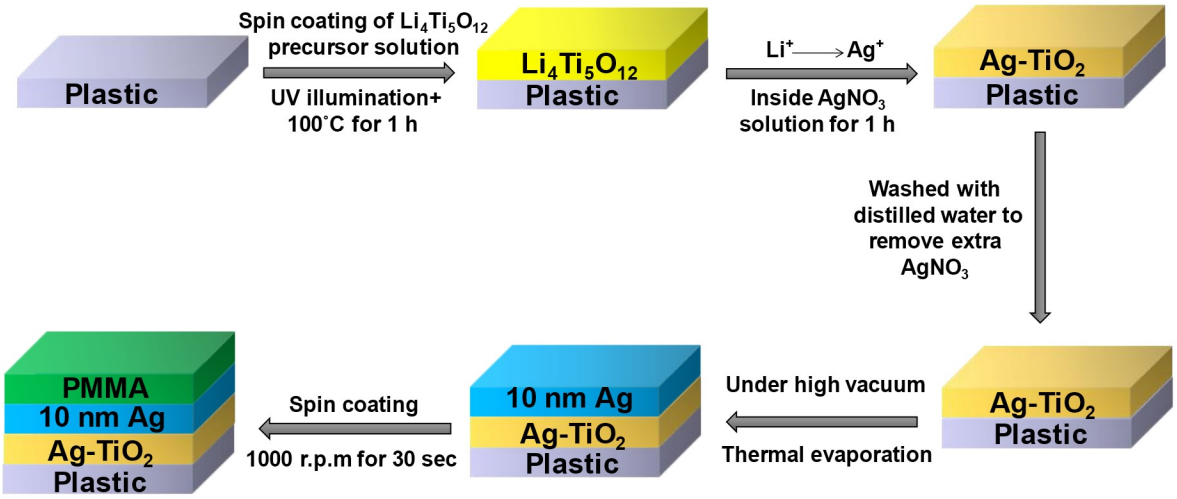

Figure 2.7 Schematic presentations of lateral growth of 10 nm Ag/Ag-TiO_2/plastic TC or THR film through low temperature annealed (100˚C) process. PMMA is used as a top layer to protect the film from oxidization.

2.3.2.1 10 nm Ag/Ag-TiO_2 TC Film based self-bias Photodetector Device

Furthermore, these fabricated 10 nm Ag/Ag-TiO_2 TC thin film have been used as transparent electrode to develop plasmonic photodetectors in a photodiode geometry which is schematically represented in **Figure 2.8**. For this device fabrication, n^+-Si has been taken as an initial substrate. At first, traditional n^+-Si substrates are properly cleaned, and the cleaning process is described in **Section 2.2.2**.100 mM precursor solution of LTO is spin coated over the clean substrate for 30 s at 3000 rpm followed by a drying process at 100°C on a hot plate. Then UV light has been illuminated by keeping the samples on a hot plate at 100°C for 1 hr. to form the crystalline LTO thin film. After that, samples are dipped in a 100 mM $AgNO_3$ solution for 1 hr. where Ag^+ of the solution are exchanged with Li^+ of LTO thin film. Following the ion-exchange procedure, the samples washed with DI water to remove any excess $AgNO_3$ from the film's surface. Finally,10 nm Ag is deposited in selected areas of the ion-exchanged thin film through a shadow mask by using a thermal evaporator technique.

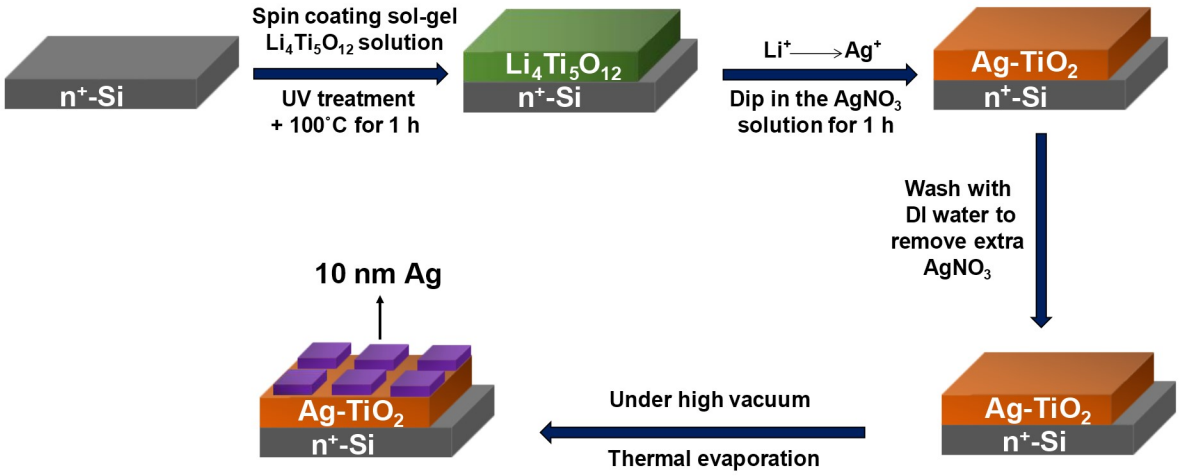

Figure 2.8 Schematic presentation of the proposed photo-diode device using fabricated 10 nm Ag/Ag-TiO_2 thin film as a transparent electrode.

2.3.3 Bimetallic Au-Ag based TC & SERS Active Thin Film

The bimetallic Au-Ag TC thin film has been fabricated on a plastic PET substrate which is schematically presented in **Figure 2.9**. The cleaning process is mentioned in **section 2.2.3**. At first, the precursor solution of as prepared SnO_2 NPs is spin-coated over the clean PET substrates for 30 s at 3000 rpm and immediately kept on a hot plate at 100°C for next 30 min. After that, film is cooled to room temperature and then spin-coated with LTO precursor solution at 3000 rpm for 30 s. Then again, film is kept in a pre-calibrated hot plate for next 1 hr. under UV light explorations. UV light of intensity ~ 0.9 mW/cm^2 is illuminated from that top side of the hotplate. This combined heating and UV illumination enable us to deposit crystalline LTO thin film at 100°C. After that, same ion-exchange procedure has been done where Ag^+ of the solution are exchanged with Li^+ of LTO thin film, to form Ag-TiO_2 thin film. The whole process is mentioned earlier in **Section 2.3.2**. The chemical reaction of this process is illustrated earlier in **Equation 2.3**. Finally, 4 nm Au thin film is deposited on the top of the film using a thermal evaporation technique to get the final Au-Ag based bimetallic TC thin film, which is also used as an active SERS substrate.

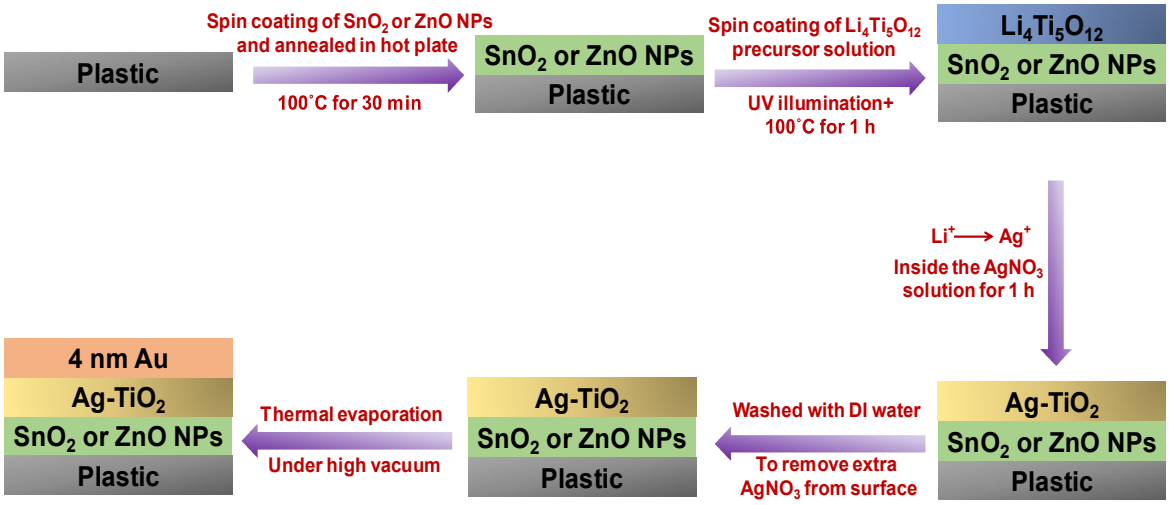

Figure 2.9 Schematic presentation of fabricated Au-Ag bimetallic TC thin film on plastic PET substrate via low temperature (100°C) synthesis route

2.3.3.1 Bimetallic Au-Ag based TC Film for Self-Bias Photodetector

The Au-Ag bi-metallic TC film is further used for the fabrication of flexible plasmonic photodetectors in a photodiode geometry (step-by-step device configuration is shown in **Figure 2.10**). Initially, plastic PET has been taken as a substrate. The whole cleaning process is mentioned in **Section 2.2.3**. Following the earlier step, we have developed Au-Ag bimetallic TC film at top of the plastic substrate which is mentioned earlier in **Section 2.3.3**. And after that a very thin layer of TiO_2 NPs is spin coated in a specific area at 3000 rpm for 30 s and followed by annealed at 100°C for 30 min to make the film crystalline. In next step, for better transport of charge carrier to the top electrode, SnO_2 NPs is coated over it at 3000 rpm for 30 s and followed by annealed at 100°C for 30 min. Finally, LiF/Al is deposited as a top metal electrode with specific mask design to develop flexible plasmonic photodetector with photo diode geometry.

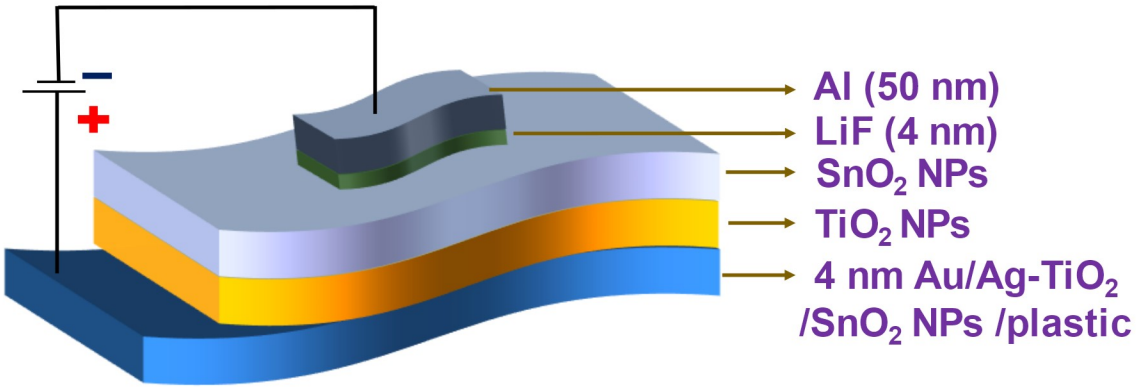

Figure 2.10 Schematic diagram of hierarchical architecture of Au-Ag TC film based flexible photodetector device.

2.3.3.2 Bimetallic Au-Ag TC Film for Plasmonic Organic Solar Cell

Furthermore, as synthesized Au-Ag bimetallic TC thin films have been used as a transparent back electrode to develop inverted plasmonic organic solar cells (device structure shown in **Figure 2.11**). Device is fabricated on plastic substrate (cleaning process is described in **Section 2.2.3)**. Firstly, using the initial step we developed an Au-Ag-based bimetallic TC film onto the plastic substrate. Next, as a HTL layer, PEDOT: PSS of 1.2 wt% is spin-coated at 1500 rpm for 40 s and annealed at 120˚C for 30 min under vacuum chamber. Now, as an active layer,15 mg/ml of only P3HT and blended P3HT:$PC_{71}BM$ (weight ratio 1:1) polymeric solution are used. Each solution is spin-coated at 1000 rpm for 60 s to get the desired thickness of the active layer and after spin coating sample is immediately annealed at 130˚C under vacuum chamber for 30 min. Next, as an ETL, SnO_2 NPs is spin-coated at 3000 rpm for 30 s and annealed at 120˚C for 30 min. Finally, 4 nm LiF/80 nm Al is deposited using thermal evaporator for top electrode. Here, LiF is used as an interfacial electron ejecting layer which also helps to reduce the overall work function of Al electrode.

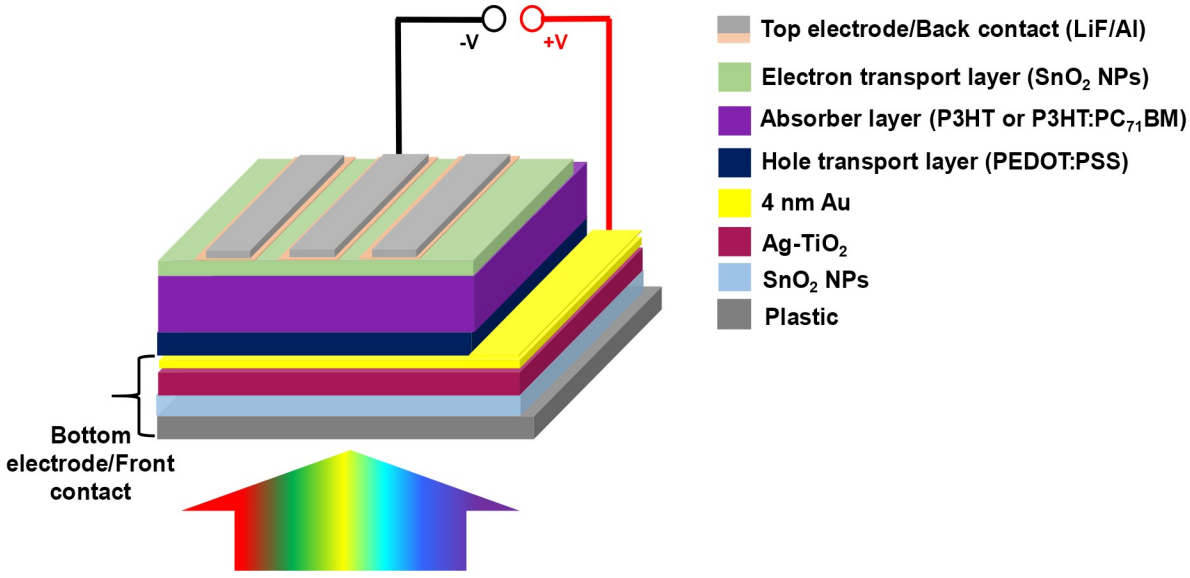

Figure 2.11 Schematic diagram of Plasmonic Organic Solar cells using Au-Ag bimetallic TC film as a back electrode.

2.4 Material Characterization

2.4.1 X-Ray Diffraction

A wide angle grazing Incidence X-Ray Diffraction (GIXRD) integrated with a multi-temperature chamber and a graphite monochromator with Cu-Kα radiation is performed using a Rigaku SmartLab system (wavelength of 0.154 nm) has been utilized to analyze the X-Ray Diffraction of as-prepared thin film samples. The generator has operated at 45 kV and 200 mA. The samples have been held on the sample holder, and the scans have been performed at a diffraction angle ranging from 20° to 60°, at a scan rate of 2°/min.

2.4.2 UV-Vis Spectroscopy

The UV-Visible spectroscopic properties of the prepared thin films have been measured using the JASCO V-770 spectrophotometer. This UV-Visible spectroscopy technique has been applied to evaluate the optical absorption of prepared plasmonic thin films.

2.4.3 Reflectance & Transmittance Spectra

Reflectance and transmittance study of plasmonic thin films have been studied by using an external quantum efficiency cum reflectance/transmission measurement set-up (Enlitech QE-R EQE).

2.4.4 Photoluminescence Spectroscopy

Photoluminescence (PL) spectra of the prepared thin films within the wavelength range of 300-550 nm have been measured using the F-4600 FLSPECTOROPHOTOMET. Using this technique, we can detect the emitted photons of plasmonic thin films at different wavelengths.

2.4.5 Surface Enhanced Raman Spectroscopy

The vibrational characteristics of SERS substrates are studied by Raman spectroscopy using an AIRIX Corp. STR 300 spectrometer, with a 532 nm excitation laser, 100× objective lens and 1200 cm^{-1} gratings. To avoid degradation of analyte biomolecules, low laser power (0.69 mW for 633 nm and 1.15 mW for 532 nm) is used for SERS study.

2.4.6 Atomic Force Microscopy

The surface morphology study of plasmonic thin films is essential to understanding the metal/dielectric interface, which plays a crucial role in the performance of thin-film photonic technologies. The rough interface acts as a transport barrier, hindering the transportation of charge carriers in semiconductors. Therefore, creating a high-quality plasmonic thin film with very low roughness is crucial. An atomic force microscopy instrument with powerful nanoscale resolution has been used to investigate the surface roughness of the prepared plasmonic thin film. The distance between the cantilever tip and the sample's surface has determined the operating mode of the atomic force microscope (AFM). The NT-MDT multimode AFM (Russia) (atomic scale resolution ~ 2 nm for HOPG), controlled by a Solver scanning microscope controller, has been used to scan the bulk surface morphology of the samples. The root mean square roughness of a plasmonic thin film has been calculated using the semi-contact mode of AFM. For this mode, a single-beam cantilever with a tip of length (l), width (w) and thickness (h) of 123 µm, 35 µm and 1.84 µm is mounted having a resonant frequency range between 240 to 255 kHz and a corresponding spring constant of 11.5 N/m.

2.4.7 High Resolution Scanning Electron Microscopy

The High-Resolution Scanning Electron Microscope (HR-SEM) is a type of electron microscope that uses a focused beam of electrons to scan the surface of a sample for image acquisition. Electrons interact with atoms in the sample, producing diverse signals that transmit information about the sample's surface topography and composition. The electron beam has been scanned in a raster pattern, and the combination of beam position and signal intensity has created an image. Generally, in SEM studies, secondary electrons generated by atoms stimulated by the electron beam have been detected using a secondary electron detector (Everhart-Thornley detector). The quantity of detectable secondary electrons, and hence the signal intensity, has been influenced by specimen topography and other factors. The HR-SEM model NANOSEM 450, FEITM, (resolution 100 nm in secondary electron imaging mode) has been utilized to examine the morphology and cross-sectional view of the samples. For the elemental analysis and color mapping, energy dispersive spectroscopy (EDX) studies have been performed using EDX analysis equipment attached with the HR-SEM instrument.

2.4.8 High Resolution Transmission Electron Microscopy

High resolution transmission electron microscopy (HR-TEM) is a method of imaging that allows the observation of a sample's crystallographic structure at the atomic level. In contrast to conventional microscopy, this does not use absorption to form images; instead, images are created through interference in the image plane. The electrons interact with the sample individually, and the electron wave passes via the imaging system, where phase change takes place. The recorded image does not directly represent the sample structure. Because of its extreme resolution, this approach is an excellent tool for exploring nanoscale material characteristics. The size of NP, particle distribution and crystallite nature of different NPs have been analyzed by HR-TEM, Tecnai G2 20 TWIN unit (point-to-point resolution 0.24 nm and a lattice resolution of 0.10 nm).

2.5 Electrical Characterization

2.5.1 Photoconductor: Current Vs Voltage (I-V) Characterization

Photoconductivity is an electro-optical phenomenon in which a material exhibits increased electrical conductivity upon absorbing EM radiation, such as UV-Vis or NIR light. Photoconductor is a two-terminal lateral device. When incident light interacts with the material, photons are absorbed by electrons in the valence band, exciting them to the conduction band and leaving behind holes. This process generates additional charge carriers in the form of electrons and holes, resulting in an overall increase in electrical conductivity. The enhancement in conductivity is thus directly attributed to photoexcitation in the carrier channel. Here, for the measurement of photoconductor, an Agilent B1500A semiconductor parameter analyzer is employed. Electrical contact with the device electrodes is established using a probe micromanipulator. All measurements are conducted under ambient atmospheric conditions. The formula for calculation of photocurrent generation is given in **Equation 2.4** and given by –

$$I_{ph} = I_{light} - I_{dark} \text{ ---------- (2.4)}$$

2.5.2 Photodiode: Current Vs Voltage (I-V) Characterization

A photodiode is a two terminal vertical device that converts incident light into an electrical current through the principle of the photoelectric effect. Unlike a photoconductor, which relies on increased conductivity due to photoexcitation, a photodiode operates as a two-terminal junction device, typically in reverse bias mode, to generate a photocurrent proportional to the intensity of incident EM radiation. When incident light interacts with the depletion region of the photodiode, photons are absorbed by electrons in the valence band, exciting them to the conduction band and generates electron-hole pairs. The built-in electric field of the depletion region facilitates the separation of these charge carriers, generating a photocurrent. This photocurrent is collected at the electrodes, leading to a measurable response. Considering the I–V curves, one can utilize the thermionic emission (TE) theory to calculate photodiode parameters. According to TE, using the experimental I-V graph we can calculate the main diode parameters such as ideality factor (n), barrier height (Φ_b), and saturation current (I_o). The relationship between I and V is represented by the following **Equations (2.5 & 2.6)[**141, 142**]**:

$$I = I_o \left[\exp\left(\frac{qV}{KT}\right) - 1\right] \text{ ---------- (2.5)}$$

$$I_o = AA^*T^2 \exp\left(-\frac{q\Phi_b}{KT}\right) \text{ ---------- (2.6)}$$

where A is the effective area of the photodiode, A^* is the effective Richardson constant, q is the electronic charge, T is the room temperature in K, and k is the Boltzmann constant.

Even though finding an ideal rectifier contact is impossible, an ideal diode has an ideality factor of 1. Higher values of n than unity are caused by a number of circumstances. The high ideality factor is often shown due to the complex interplay of carrier generation, recombination, mobility, surface effects, and temperature. These factors introduce deviations from the ideal diode equation. The experimental values of Φ_b and n are determined by **Equations** (**2.7 & 2.8**) as follows[141, 143]:

$$\Phi_b = \frac{KT}{q} \ln\left(\frac{AA^*T^2}{I_0}\right) \text{ ---------- (2.7)}$$

$$n = \frac{q}{KT}\left(\frac{dV}{d\ln I}\right) \text{ ---------- (2.8)}$$

For the measurement of the photodiode's I-V characteristics, the same Agilent B1500A semiconductor parameter analyzer is employed. Electrical contact with the device terminals is established using a probe micromanipulator. All measurements are conducted under ambient atmospheric conditions to evaluate the device's performance in real-world environments.

2.5.3 Photovoltaics devices: Current Density Vs Voltage (J-V) Characterization

The J-V characteristics of the fabricated solar cells are measured in both dark and illuminated conditions to evaluate their performance. These measurements are conducted using a solar simulator (Photoemission Inc., USA, Class AAA) under the standard Air Mass 1.5 Global (AM 1.5G) solar spectrum at room temperature, with an Keithley 2450 source meter applying as an external potential bias. In forward bias, electrons are injected from the photoanode into the device, while in reverse bias, electrons are injected from the counter electrode side. An ideal solar cell exhibits typical diode behavior under dark condition which is shown in

Figure 2.12 (red line). At low applied voltage, minimal or no current flows due to the low charge carrier density in the dark. As the applied voltage increases, charge density rises, leading to an upward shift in the quasi-Fermi level within the metal oxide. When the quasi-Fermi level aligns with the conduction band of the active material, electron transport to the back electrode becomes unhindered, increasing the dark current. This behavior confirms that dark current is primarily governed by electron-hole recombination, which dictates charge carrier dynamics in the absence of illumination.

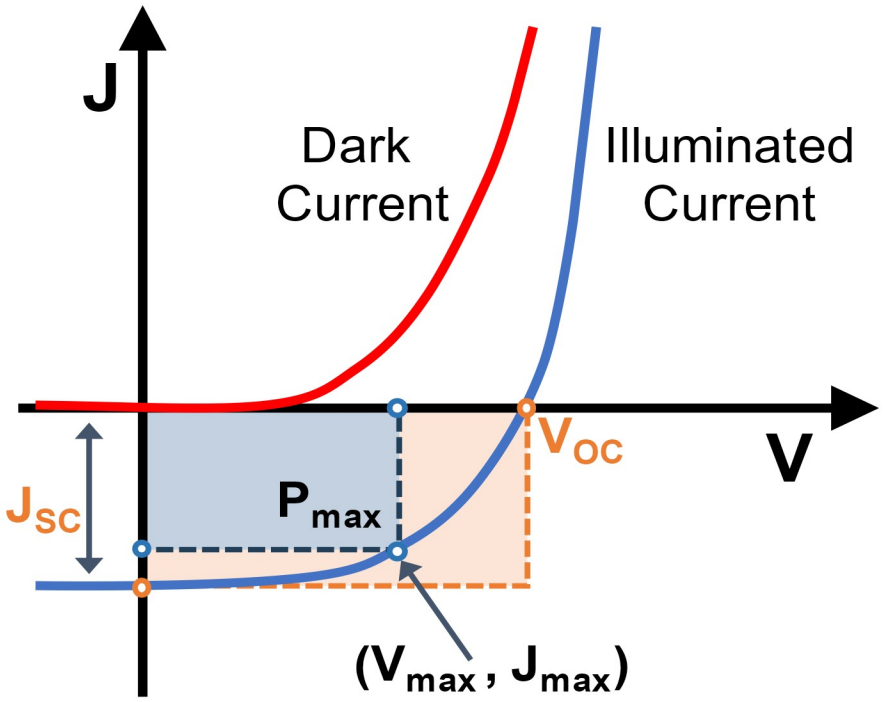

Figure 2.12 J-V curve of typical photovoltaics under dark (red line) and light (blue) illumination.

Under illumination, photocurrent is generated and flows opposite to the dark current, as shown in

Figure 2.12 (blue line). The J-V characteristics are governed by two competing processes: photocurrent generation and electron-hole recombination. At a low applied potential, most charge carriers are collected before recombination, resulting in a nearly constant photocurrent. As the applied potential increases, recombination dominates, reducing the photocurrent until it reaches zero, which is termed as open-circuit voltage (V_{oc}). At zero bias,

the photocurrent is termed the short-circuit current density (J_{sc}). The maximum of the power curve is called the maximum power point (P_{max}), and the corresponding voltage and current are denoted as J_{max} and V_{max}, described with **Equation 2.9.** The power conversion efficiency (PCE) is a key parameter for evaluating solar cell performance and is given by -

$$\mathbf{PCE} = \frac{P_{max}}{P_{in}} = \frac{J_{max} \times V_{max}}{P_{in}} \text{ ---------- (2.9)}$$

where P_{in} is the illuminated light intensity (100 mW/cm^2)

Another crucial parameter of a solar cell is the fill factor (FF), which represents the squareness of the I-V curve and is defined as (**Equation 2.10**)-

$$\mathbf{FF} = \frac{J_{max} \times V_{max}}{J_{sc} \times V_{oc}} \text{ -------- (2.10)}$$

Finally, utilizing all the factor, PCE is determined using **Equation 2.11** and is given by-

$$\mathbf{PCE} = \frac{J_{sc} \times V_{oc} \times FF}{P_{in}} \text{ -------- (2.11)}$$

2.5.4 Current Vs Time (I-t) Characterization

Transient photo response is another key parameter of a photodetector that implies how fast a device can respond to light and how promptly it can return to its original stage for detecting the next signal. Here, the transient response of photodetector device has been measured by measuring the current vs time (I-t) behaviour of the device. This is a two-probe measurement, and it has been utilized to calculate the response time (rise time and fall time) of the device under the influence of illumination of light. The time intervals needed for the photocurrent to increase from 10% to 90% of its peak value (τ_r) and for the response to decrease from 90% to 10% of its peak value (τ_f) are always used to define the device rise time (τ_r) and fall time (τ_f).

2.5.5 Quantum Efficiency Measurement

Quantum efficiency measures the ratio of collected charge carrier in the form of electrons to the number of incident photons. Quantum efficiency can be expressed as external quantum

efficiency (EQE) and internal quantum efficiency (IQE). The EQE measures how efficiently a photovoltaics or photodetector device converts incident photons into electrical current. The external quantum efficiency of a device generally follows the relation (**Equation 2.12**) [107]–

$$\mathbf{EQE\ (\%) = \eta_{abs} \times \eta_{gen} \times \eta_{coll}} \quad \text{---------- (2.12)}$$

Where η_{abs}, η_{gen} and η_{coll} are the absorption efficiency, e^{-}- h^{+} charge generation efficiency and charge collection efficiency of the charge transport layer, respectively.

Among these, η_{abs} has significant wavelength dependence. When a device is illuminated with light, electromagnetic waves flow through many layers of thin film devices and during this process, photons may be absorbed, reflected by the interface, followed by repeated reflections, or transmitted through the device. As a result, EQE tends to follow materials' optical absorption properties. However, this value includes photons lost through optical transmission and reflection.

While IQE measure excluded the losses due to the reflection of light, as a result IQE value is always greater compare to EQE value. IQE can be measured or extract from EQE value by using **Equation 2.13**-

$$\mathbf{IQE} = \frac{\mathbf{EQE}}{\mathbf{1-R}} \text{ ---------- (2.13)}$$

where R is the reflectance of the device